Since January 2020 Elsevier has created a COVID-19 resource centre with free information in English and Mandarin on the novel coronavirus COVID-19. The COVID-19 resource centre is hosted on Elsevier Connect, the company's public news and information website.

Veterinary Microbiology 166 (2013) 123–137

Contents lists available at SciVerse ScienceDirect

Veterinary Microbiology

journal homepage: www.elsevier.com/locate/vetmic

Pathogenicity of porcine G9P[23] and G9P[7] rotaviruses in piglets

Ha-Hyun Kim [a,d,1], Jun-Gyu Park [a,1], Jelle Matthijnssens [b], Hyun-Jeong Kim [a], Hyung-Jun Kwon [a,c], Kyu-Yeol Son [a], Eun-Hye Ryu [a], Deok-Song Kim [a], Woo Song Lee [c], Mun-Il Kang [a], Dong-Kun Yang [d], Ju-Hwan Lee [e], Su-Jin Park [c], Kyoung-Oh Cho [a,*]

[a] Laboratory of Veterinary Pathology, College of Veterinary Medicine, Chonnam National University, Gwangju 500-757, Republic of Korea
[b] Laboratory of Clinical and Epidemiological Virology, Department of Microbiology and Immunology, Rega Institute for Medical Research, University of Leuven, Leuven, Belgium
[c] Eco-Friendly Biomaterial Research Center and AI Control Material Research Center, Korea Research Institute of Bioscience and Biotechnology, Jeongeup 580-185, Republic of Korea
[d] Animal and Plant Quarantine Agency, Anyang, Gyonggi-do 430-757, Republic of Korea
[e] Chonnam National University Veterinary Teaching Hospital, Gwangju 500-757, Republic of Korea

ARTICLE INFO

Article history:
Received 27 January 2013
Received in revised form 5 May 2013
Accepted 22 May 2013

Keywords:
Group A rotaviruses
G9 genotype
Pathogenicity
Piglets
Experimental model

ABSTRACT

G9 group A rotaviruses (RVAs) are considered important pathogens in pigs and humans, and pigs are hypothesized to be a potential host reservoir for human. However, intestinal and extra-intestinal pathogenicity and viremia of porcine G9 RVAs has remained largely unreported. In this study, colostrum-deprived piglets were orally infected with a porcine G9P[23] or G9P[7] strain. Histopathologically, both strains induced characteristic small intestinal lesions. Degeneration and necrosis of parenchymal cells were observed in the extra-intestinal tissues, but most predominantly in the mesenteric lymph nodes (MLNs). RVA antigen was continuously detected in the small intestinal mucosa and MLNs, but only transiently in cells of the liver, lung, and choroid plexus. Viral RNA levels were much higher in the feces and the MLNs compared to other tissues. The onset of viremia occurred at day post infection (DPI) 1 with the amount of viral RNA reaching its peak at DPI 3 or 5, before decreasing significantly at DPI 7 and remaining detectable until DPI 14. Our data suggest that porcine G9 RVAs have a strong small intestinal tropism, are highly virulent for piglets, have the ability to escape the small intestine, spread systemically via viremia, and replicate in extra-intestinal tissues. In addition, MLNs might act as a secondary site for viral amplification and the portal of systemic entry. These results add to our understanding of the pathogenesis of human G9 RVAs, and the validity of the pig model for use with both human and pig G9 RVAs in further studies.

1. Introduction

Group A rotaviruses (RVAs) are one of the 8 rotavirus species recognized in the *Reoviridae* family (Matthijnssens et al., 2012), and are responsible for severe gastroenteritis, primarily in children <5 years of age as well as the young of many mammalian species (Estes and Kapikian, 2007; Gentsch et al., 2005). In humans, RVA infections result in

* Corresponding author at: Global-bio Human Resource Center for Disease-control, Laboratory of Veterinary Pathology, College of Veterinary Medicine, Chonnam National University, Gwangju 500-757, Republic of Korea. Tel.: +82 62 530 2845; fax: +82 62 530 2809.
E-mail address: choko@chonnam.ac.kr (K.-O. Cho).
[1] These authors contributed equally to this work.

0378-1135/$ – see front matter © 2013 Elsevier B.V. All rights reserved.
http://dx.doi.org/10.1016/j.vetmic.2013.05.024

the death of 453,000 infants and young children each year, mostly in developing countries (Tate et al., 2012). The genome of RVA consists of 11 segments of double-stranded RNA enclosed in a triple layered particle (Estes and Kapikian, 2007). Most segments encode a single polypeptide, allowing the virus to express six structural (VP1-VP4, VP6, and VP7) and five or six nonstructural proteins (NSP1-NSP6) (Estes and Kapikian, 2007). Recently, a classification system encompassing all 11 genome segments was developed using nucleotide cut-off values and phylogenetic analyses. The notation Gx-P[x]-Ix-Rx-Cx-Mx-Ax-Nx-Tx-Ex-Hx is used for the VP7-VP4-VP6-VP1-VP2-VP3-NSP1-NSP2-NSP3-NSP4-NSP5/6 encoding gene segments, respectively (Matthijnssens et al., 2008a,b). This system offers international standardization to analyze RVA interspecies evolutionary relationships, gene reassortment events, functional gene linkage in reassortant progeny, emergence of new RVA strains, RVA host range restriction, and virulence (Matthijnssens et al., 2008a,b).

Porcine RVA strains are highly divergent, and multiple G-genotypes (G1-G6, G8-G12, G26) and P-genotypes (P[1], P[5]-P[7], P[11], P[13], P[19], P[23], P[26], P[27], P[32]) have been described in pigs (Collins et al., 2010; Martella et al., 2010). Complete genome analyses have revealed that several virus gene segments typically found in pig RVA strains and Wa-like human RVA strains have a common ancestor (Matthijnssens et al., 2008a). Porcine RVAs are considered important pathogens due to their economic impact on the pig industry and are a significant reservoir for human RVAs (Kim et al., 2010; Matthijnssens et al., 2008a, 2010b; Zeller et al., 2012). G9 RVA strains have so far been detected only in pigs and humans, and pigs are hypothesized to be a potential reservoir for human G9 RVAs (Mascarenhas et al., 2007; Matthijnssens et al., 2010a). Since G9 RVAs were first detected in diarrhoeal samples of children in Córdoba, Argentina, and in Washington State during 1980, G9 RVA strains belonging to lineage 3 have now spread throughout the world and are now recognized as the fifth most globally important human genotype (Barril et al., 2006; Cao et al., 2008; Matthijnssens et al., 2010a; Phan et al., 2007; Santos and Hoshino, 2005). These lineage 3 human G9 RVA strains have been shown to be both phylogenetically and antigenically related to one the first described porcine G9 RVA strains A2 (Hoshino et al., 2005). In South Korean pigs, the G9 genotype in combination with the P[7] and P[23] genotypes has been isolated and identified as the third most important genotype after G5P[7] and G8P[7] (Kim et al., 2010). Most recently, full-length genomic analysis of porcine G9P[23] and G9P[7] RVAs revealed that these porcine G9 RVAs possess typical porcine genotype constellations: G9–P[23]/P[7]–I5–R1–C1–M1–A8–N1–T1–E1–H1 (Kim et al., 2012a). This report provided basic genetic information of G9 RVA strains, which are increasing in prevalence and are important in both humans and pigs.

RVA infection has been thought to be restricted to the gastrointestinal tract, typically the small intestine. However, accumulating evidence suggests that RVA escapes the gastrointestinal tract and spreads to the extra-intestinal organs in both human and animals. For example, RVA antigen and viral RNA have been detected in serum samples from children with RVA diarrhea, indicating that antigenemia and possibly viremia could occur during RVA infection (Blutt et al., 2003; Chiappini et al., 2005; Fischer et al., 2005). In children who died during RVA infection, RVA antigens and viral RNA were detected in the extra-intestinal organs and tissues including the central nervous system, liver, lung, spleen, heart, kidney, testis, and bladder (Blutt and Conner, 2007; Lynch et al., 2001; Pager et al., 2000; Ramig, 2004; Riepenhoff-Talty et al., 1996; Zheng et al., 1991). It has been clearly demonstrated that RVAs cause not only gastrointestinal but also systemic infections in experimental animal models (Ciarlet et al., 2002; Crawford et al., 2006; Fenaux et al., 2006; Kim et al., 2011, 2012b; Petersen et al., 1998).

Although RVAs are believed to cause intestinal and extra-intestinal pathology in humans and animals, the pathogenicity of G9 bearing RVA strains has to date remained largely unreported. Therefore, this prompted us to investigate the ability of porcine G9 RVA strains to cause intestinal and extra-intestinal lesions and viremia. To explain in detail how G9 RVAs replicate, spread and cause disease in pigs, in the present study we investigated intestinal and extra-intestinal virus spread and viremia, as well as the pathology of intestinal organs, extra-intestinal organs and tissues in colostrum-deprived piglets orally inoculated with a porcine G9P[7] or G9P[23] RVA strain.

2. Materials and methods

2.1. Virus inoculum

The porcine G9 RVA strains (RVA/Pig-tc/KOR/PRG942/2006/G9P[23] and RVA/Pig-tc/KOR/PRG9121/2006/G9P[7]) were isolated from diarrheic fecal samples collected from piglets in South Korea during 2006 (Kim et al., 2012a). These strains were passaged eight times in TF-104 cells (a cloned derivative of MA-104 monkey kidney cells), including isolation, adaptation, and triple plaque purification (Kim et al., 2012a). The genome constellations of the Korean porcine G9 RVA strains (RVA/Pig-tc/KOR/PRG942/2006/G9P[23] and RVA/Pig-tc/KOR/PRG9121/2006/G9P[7]) were determined as G9–P[23]/P[7]–I5–R1–C1–M1–A8–N1–T1–E1–H1, being only different in the VP4 genotype (P[23] for PRG942 and P[7] for PRG9121) (Kim et al., 2012a). Virus titers were expressed as fluorescent focus units (FFU) per milliliter. The virus titers of each strain were determined to 1.3×10^7 FFU/ml for PRG942 (G9P[23]) and 1.0×10^7 FFU/ml for PRG9121 (G9P[7]) by a cell culture immunofluorescence assay (IFA) (Kim et al., 2011). The supernatant from mock-infected TF-104 cell cultures was prepared for colostrum-deprived piglets as mock-inoculated controls. In addition, PRG942 (G9P[23]) and PRG9121 (G9P[7]) strains were inactivated by a chloroform treatment, and used to inoculate colostrum-deprived piglets to exclude detection of residual RVA antigen or RNA from the inocula after inoculation (Kim et al., 2011).

2.2. Animals and experimental design

A total of twenty colostrum-deprived piglets obtained from sows by hysterectomy were used to evaluate the

Table 1
Diarrhea incidence, virus shedding, and viremia in piglets inoculated with PRG942 (G9P[23]) strain.

Piglet no.	Inoculum	DPI at euthanasia	Diarrhea onset DPI (duration)	Feces		Nasal swab		Serum	
				RT-PCR onset DPI (duration)	Nested PCR onset DPI (duration)	RT-PCR onset DPI (duration)	Nested PCR onset DPI (duration)	RT-PCR	Nested PCR
1–2	PRG942	1	1 (1)	1 (1)	1 (1)	None	None	–	+
3–4	PRG942	3	1 (3)	1 (3)	1 (3)	2 (2)	2 (2)	+	+
5	PRG942	5	1 (5)	1 (5)	1 (5)	3 (3)	2 (4)	+	+
6	PRG942	7	1 (7)	1 (7)	1 (7)	3 (3)	2 (4)	–	–
7	PRG942	14	1 (8)	1 (8)	1 (10)	3 (4)	2 (5)	–	–
8	Mock[a]	2	None	None	None	None	None	None	None
9	Inactivated PRG942[b]	3	None	None	None	None	None	None	None

[a] Mock inoculation with supernatant from mock-infected TF-104 cell cultures.
[b] Inoculation with chloroform-inactivated PRG942 strain.

Table 2
Diarrhea incidence, virus shedding and viremia in piglets inoculated with PRG9121 (G9P[7]) strain.

Piglet no.	Inoculum	DPI at euthanasia	Diarrhea onset DPI (duration)	Feces		Nasal swab		Serum	
				RT-PCR onset DPI (duration)	Nested PCR onset DPI (duration)	RT-PCR onset DPI (duration)	Nested PCR onset DPI (duration)	RT-PCR	Nested PCR
1–2	PRG9121	1	1 (1)	1 (1)	1 (1)	None	None	–	–
3–4	PRG9121	3	1 (3)	1 (3)	1 (3)	2 (2)	2 (2)	+	+
5	PRG9121	5	1 (5)	1 (5)	1 (5)	3 (3)	2 (3)	+	+
6	PRG9121	7	1 (7)	1 (7)	1 (7)	3 (3)	2 (4)	–	–
7	PRG9121	14	1 (8)	1 (8)	1 (10)	3 (3)	3 (3)	–	–
8	Mock[a]	2	None	None	None	None	None	None	None
9	Inactivated PRG9121[b]	3	None	None	None	None	None	None	None

[a] Mock inoculation with supernatant from mock-infected TF-104 cell cultures.
[b] Inoculation with chloroform-inactivated PRG9121 strain.

pathogenicity of the porcine G9 RVA strains PRG942 (G9P[23]) and PRG9121 (G9P[7]). Two groups of seven 3-day-old piglets were orally inoculated with 4 ml of the cell culture supernatant containing a virus titer of 1.3×10^7 FFU/ml (G9P[23] PRG942) and 1.0×10^7 FFU/ml (G9P[7] PRG9121). Two piglets were inoculated orally with 4 ml of mock-infected TF-104 tissue culture supernatant. Chloroform-inactivated PRG942 (G9P[23]) and PRG9121 (G9P[7]) strains were orally inoculated into two piglets each. Animals were fed autoclaved commercial piglet formula during the course of the study.

The virus-inoculated piglets were euthanized at day post-inoculation (DPI) 1, 3, 5, 7, and 14 (Tables 1 and 2). The mock-inoculated and inactivated virus-inoculated piglets were euthanized at DPI 2 and 3, respectively. All studies were approved by the University Animal Care Committee (CNU IACUC-YB-R-2009-15).

2.3. Sample collection and processing

Fecal and nasal samples were collected daily from each piglet before and after inoculation, whereas blood samples were collected at euthanasia. At sacrifice, the intestinal tracts were removed from the abdominal cavities and the small and large intestinal contents were collected.

The intestinal segment, mesenteric lymph node (MLN), nasal turbinate, trachea, lung, liver, spleen, kidney, heart, brain, and choroid plexus were excised from each piglet, and each tissue was immediately placed in 10% buffered formalin for histological examination. Formalin-fixed and paraffin-embedded sections from each organ and tissue were stained with Mayer's hematoxylin and eosin (Kim et al., 2011). To detect RVA antigens by IFA, each intestinal and extra-intestinal organ was sampled from virus-inoculated and mock-inoculated piglets, embedded in optimal cutting temperature (OCT) compound, immediately snap-frozen in liquid nitrogen, and stored at −80 °C. For RT-PCR and real-time RT-PCR, all samples collected from experimental piglets were immediately snap-frozen in liquid nitrogen, and stored at −80 °C until use.

2.4. Evaluation of histopathology

Histopathological findings were evaluated in small intestinal sections of piglets of both infected groups (sacrificed at DPI 1, 3, 5, 7 and 14), mock-inoculated piglets, and the inactivated virus-inoculated piglets. Stained sections were visualized by light microscopy and villi atrophy of the small intestine was examined in histological sections of the duodenum, jejunum, and ileum. The histological evaluation was performed in a blinded fashion on coded samples and mean lesion changes were determined by examining 10 randomly selected villi and crypts of histological sections as described previously (Kim et al., 2011; Park et al., 2007). The histopathological findings of the small intestine were graded according to the average villi/crypt (V/C) ratio plus the grade of epithelial cell desquamation. The grade was measured as follows: V/C ratio, 0 = normal; (V/C ≧ 6:1), 1 = mild; (V/C = 5.0–5.9:1), 2 = moderate; (V/C = 4.0–4.9:1), 3 = marked;

(V/C = 3.0–3.9:1), 4 = severe; (V/C ≦ 3.0:1), and desquamation grade, 0 = normal (no desquamation), 1 = mild (a few desquamated cells of tip villous epithelium), 2 = moderate (desquamation of upper villous epithelium), 3 = marked (desquamation of lower villous epithelium), 4 = severe (desquamation of crypt epithelium) (Kim et al., 2011; Park et al., 2007).

2.5. Detection of rotavirus antigen by IFA

IFA was performed in each tissue and organ sampled from sacrificed piglets for the detection of RVA antigen as described previously (Ciarlet et al., 2002; Kim et al., 2011). Cut frozen sections were fixed in 100% cold acetone for 10 min and allowed to completely air dry. Slides were rinsed twice with phosphate buffered saline (PBS, pH 7.2), and incubated for 2 h at room temperature (RT) with a 1:100 dilution of monoclonal antibodies against the VP6 protein of the porcine RVA strain OSU in PBS (pH 7.2). Slides were rinsed twice with PBS (pH 7.2) and incubated with a 1:100 dilution of goat anti-mouse Ig conjugated to fluorescein isothiocyanate (Jackson ImmunoResearch Labs, Baltimore, MD, USA) in PBS (pH 7.2) for 1 h at room temperature (RT). Following incubation, the slides were rinsed twice with PBS (pH 7.2). Slides were incubated with 500 mM solution of propidium iodide diluted with PBS (pH 7.2) for 10 min at RT as a nucleic acid stain. Slides were rinsed twice with PBS (pH 8.0) and covered with 60% glycerin in PBS (pH 8.0) with glass cover slips. Fluorescence was examined under ultraviolet (UV) light illumination with a Leica microscope (Leica Microsystems, Wetzlar, Germany). To calculate the number of antigen-positive cells in the tissues or organs, 10 fields per section were analyzed using a 40× objective and a 10× eyepiece, yielding a final magnification of 400×. The antigen distribution in the each tissue and organ was evaluated based on the number of antigen-positive, and was measured as follows: 0 = no positive cells, 1 = one to two positive cells, 2 = three to five positive cells scattered in tissue, 3 = many positive cells in tissue, 4 = positive in most tissue.

2.6. Detection of viral RNA by RT-PCR and nested PCR

To detect viral RNA in the feces, nasal swabs, and serum specimens sampled from virus-infected piglets and mock-inoculated animals, RT-PCR and nested PCR was employed with a primer pair specific to the VP6 gene of RVAs as described previously (Kim et al., 2011).

2.7. Quantification of viral RNA by real time RT-PCR

A one-step real-time RT-PCR assay was performed with a primer pair specific to the VP6 gene of RVAs to quantify the RNA of RVA in the samples from each piglet as described previously (Kim et al., 2011). Each sample from the feces, serum, MLN, liver, lung, choroid plexus, and nasal swab was individually weighed prior to processing. All tissue samples from piglets were homogenized or vortexed at a 1:10 dilution in PBS (pH 7.2) and centrifuged (tissues 13,000 × *g* for 3 min; fecal samples 5000 × *g* for 10 min). The supernatants of centrifuged samples were collected and stored at −80 °C prior to analysis. Total RNA was extracted in the supernatants.

The one-step real-time RT-PCR was performed using a Rotor-Gene Real-Time Amplification system (Corbett Research, Mortlake, Australia) and SensiMix one-step RT-PCR kit with SYBR Green (Quantace, London, UK) as described previously (Kim et al., 2011). Each real-time RT-PCR reaction was prepared in a final volume of 25 μl containing 5 μl of RNA template, 12.5 μl SensiMix one-step mixture, 1 μl each of 0.5 μM forward and reverse primers (final concentration of each primer: 20 nM), 0.5 μl of 50× SYBR Green solution (final concentration: 1×), 0.5 μl of RNase inhibitor (final concentration: 10 units), 0.5 μl of $MgCl_2$ (final concentration: 4.0 mM), and 4 μl of RNase free water. Reverse transcription was carried out at 50 °C for 30 min, followed by the activation of the hot-start DNA polymerase at 95 °C for 15 min and 40 cycles of three-step at 95 °C for 15 s, 51 °C for 30 s, and 72 °C for 1 min.

Rotorgene 2000® software was used for the calculation of the amount of RVA RNA in the samples. Quantitation of viral RNA was carried out using a standard curve derived from serial 10-fold dilutions of complementary RNA (cRNA) generated by reverse transcription of in vitro transcribed control RNA. The threshold was automatically defined in the initial exponential phase, reflecting the highest amplification rate. A direct relationship between the cycle number and the log concentration of RNA molecules initially present in the RT-PCR reaction was evident regarding the crossing points resulting from the amplification curves and this threshold. Rotorgene 2000® software was used to allow the determination of the concentration of RNA present in the samples by linear regression analysis (Kim et al., 2011).

3. Results

3.1. Clinical signs, fecal and nasal virus shedding, and viremia caused by porcine G9 RVA strains in piglets

Both strains caused diarrhea in all inoculated piglets at DPI 1, which persisted until DPI 8 (Tables 1 and 2). Neither the chloroform-inactivated virus nor the mock-inoculum induced diarrhea in the piglets (Tables 1 and 2). The virus-inoculated piglets did not show any other clinical signs in addition to diarrhea. These results indicated that both G9 RVA strains are able to induce diarrhea in piglets.

By RT-PCR and nested PCR, fecal virus shedding from piglets inoculated with each strain was detected at DPI 1 and persisted to DPI 8 and DPI 10 (Tables 1 and 2). Nasal shedding of both strains was detected at DPI 2 or 3 by RT-PCR, whereas nested PCR enabled detection at DPI 2 (G9P[23] PRG942 strain) and DPI 2 or 3 (G9P[7] PRG9121 strain). The duration of nasal virus shedding was 2–4 days by RT-PCR, and 2–5 days (G9P[23] PRG942) or 2–4 days (G9P[7] PRG9121) by nested PCR (Tables 1 and 2). Serum specimens were sampled from sequentially euthanized piglets. RVA RNA was detected in the sera from piglets inoculated with each strain at DPI 3 and 5 by RT-PCR (Tables 1 and 2). By nested PCR, viral RNA of strain PRG942 (G9P[23]) was present in the sera at DPI 1 and persisted to

Table 3
Histopathological findings in the small intestine of piglets inoculated with PRG942 (G9P[23]) strain.

Piglet No.	Inoculum	DPI at euthanasia	Duodenum		Jejunum		Ileum	
			Lesion score[a]	RVA Ag distribution[b]	Lesion score[a]	RVA Ag distribution[b]	Lesion score[a]	RVA Ag distribution[b]
1	PRG942	1	1.1	2.6	0.8	2.0	1.0	1.4
2	PRG942	1	1.3	2.8	1.0	1.5	0.9	1.8
3	PRG942	3	2.9	3.2	2.5	2.8	2.4	2.8
4	PRG942	3	3.0	3.0	3.2	3.0	2.6	2.8
5	PRG942	5	3.1	2.4	3.2	1.8	2.6	2.0
6	PRG942	7	3.4	2.5	3.3	2.0	3.2	1.6
7	PRG942	14	3.0	0.6	2.7	0.4	2.8	0.4
8	Mock	2	0	0	0	0	0	0
9	Inactivated PRG942	3	0	0	0	0	0	0

[a] The small intestinal changes were scored according to the average villi/crypt (V/C) ratio plus the grade of epithelial cell desquamation, which was measured as follows: V/C ratio, 0 = normal (V/C ≧ 6:1), 1 = mild (V/C = 5.0–5.9:1), 2 = moderate (V/C = 4.0–4.9:1), 3 = marked (V/C = 3.0–3.9:1), 4 = severe (V/C ≦ 3.0:1) and desquamation grade, 0 = normal (no desquamation), 1 = mild (cuboidal attenuation of tip villous epithelium), 2 = moderate (desquamation of upper villous epithelium), 3 = marked (desquamation of lower villous epithelium), 4 = severe (desquamation of crypt epithelium).

[b] The antigen distribution in the small intestine was evaluated based on the number of antigen-positive cells in the villi, and was measured as follows: 0 = no positive cells, 1 = one to two positive cells in the villi, 2 = three to five positive cells scattered in the villi, 3 = many positive cells in the villi, 4 = positive in almost all epithelial cells in the tip and upper part of the villi.

DPI 5, whereas viral RNA of strain PRG9121 (G9P[7]) was detected in the sera at DPI 3 and 5 (Tables 1 and 2). Fecal and nasal virus shedding, and viremia were not detected in the inactivated G9 RVAs- and mock-inoculated piglets by RT-PCR and nested PCR (Tables 1 and 2). These results imply that both strains can induce virus shedding through feces and nostrils, as well as causing viremia in piglets.

3.2. Intestinal histopathology caused by porcine G9 RVA strains in piglets

To determine the sequential histopathological changes in the small intestines of piglets orally inoculated with PRG942 (G9P[23]) or PRG9121 (G9P[7]) and euthanized at DPI 1, 3, 5, 7, and 14, each small intestinal fragment was sampled, and multiple cross sections of each fragment were histopathologically evaluated.

Sequential histopathological lesion changes in the small intestines of piglets inoculated with either PRG942 (G9P[23]) or PRG9121 (G9P[7]) are summarized in Tables 3 and 4. Both strains induced histopathological changes in the small intestinal mucosa at DPI 1, including villous atrophy and crypt hyperplasia (Figs. 1 and 2). Over time, these mucosal changes gradually increased in all parts of the small intestine until DPI 7 and then decreased at DPI 14. Although the villous length was restored at DPI 14, a marked crypt hyperplasia was sustained, resulting in the high histopathological lesion score at DPI 14. As time elapsed, villous epithelial desquamation caused by the degeneration or necrosis of the villi lining the epithelium, and infiltration of lymphoid cells in the lamina propria of the villi tended to increase. No lesions were observed in duodenum, jejunum and ileum of small intestines sampled from either inactivated virus- or mock-inoculated piglets (Figs. 1 and 2, Tables 3 and 4).

3.3. Antigen localization of porcine G9 RVA strains in small intestines of piglets

IFA was performed on samples from the duodenum, jejunum, and ileum of piglets inoculated with either the PRG942 (G9P[23]) or PRG9121 (G9P[7]) RVA strain to assess

Table 4
Histopathological findings in the small intestine of piglets inoculated with PRG9121 (G9P[7]) strain.

Piglet No.	Inoculum	DPI at euthanasia	Duodenum		Jejunum		Ileum	
			Lesion score[a]	RVA Ag distribution[b]	Lesion score[a]	RVA Ag distribution[b]	Lesion score[a]	RVA Ag distribution[b]
1	PRG9121	1	1.9	2.4	1.9	2.2	1.6	2.2
2	PRG9121	1	2.0	2.8	1.8	2	1.7	2.6
3	PRG9121	3	2.8	3.2	3.2	2.8	2.4	3.2
4	PRG9121	3	3.3	3.6	3.1	3.2	2.9	3.0
5	PRG9121	5	3.5	2.6	3.2	2.8	3.1	2.2
6	PRG9121	7	3.4	2.0	3.3	2.0	3.2	1.8
7	PRG9121	14	3.2	1.0	3.1	0.8	2.9	1.0
8	Mock	2	0	0	0	0	0	0
9	Inactivated PRG9121	3	0	0	0	0	0	0

[a] The small intestinal changes were scored according to the average villi/crypt (V/C) ratio plus the grade of epithelial cell desquamation, which was measured as follows: V/C ratio, 0 = normal (V/C ≧ 6:1), 1 = mild (V/C = 5.0–5.9:1), 2 = moderate (V/C = 4.0–4.9:1), 3 = marked (V/C = 3.0–3.9:1), 4 = severe (V/C ≦ 3.0:1) and desquamation grade, 0 = normal (no desquamation), 1 = mild (cuboidal attenuation of tip villous epithelium), 2 = moderate (desquamation of upper villous epithelium), 3 = marked (desquamation of lower villous epithelium), 4 = severe (desquamation of crypt epithelium).

[b] The antigen distribution in the small intestine was evaluated based on the number of antigen-positive cells in the villi, and was measured as follows: 0 = no positive cells, 1 = one to two positive cells in the villi, 2 = three to five positive cells scattered in the villi, 3 = many positive cells in the villi, 4 = positive in almost all epithelial cells in the tip and upper part of the villi.

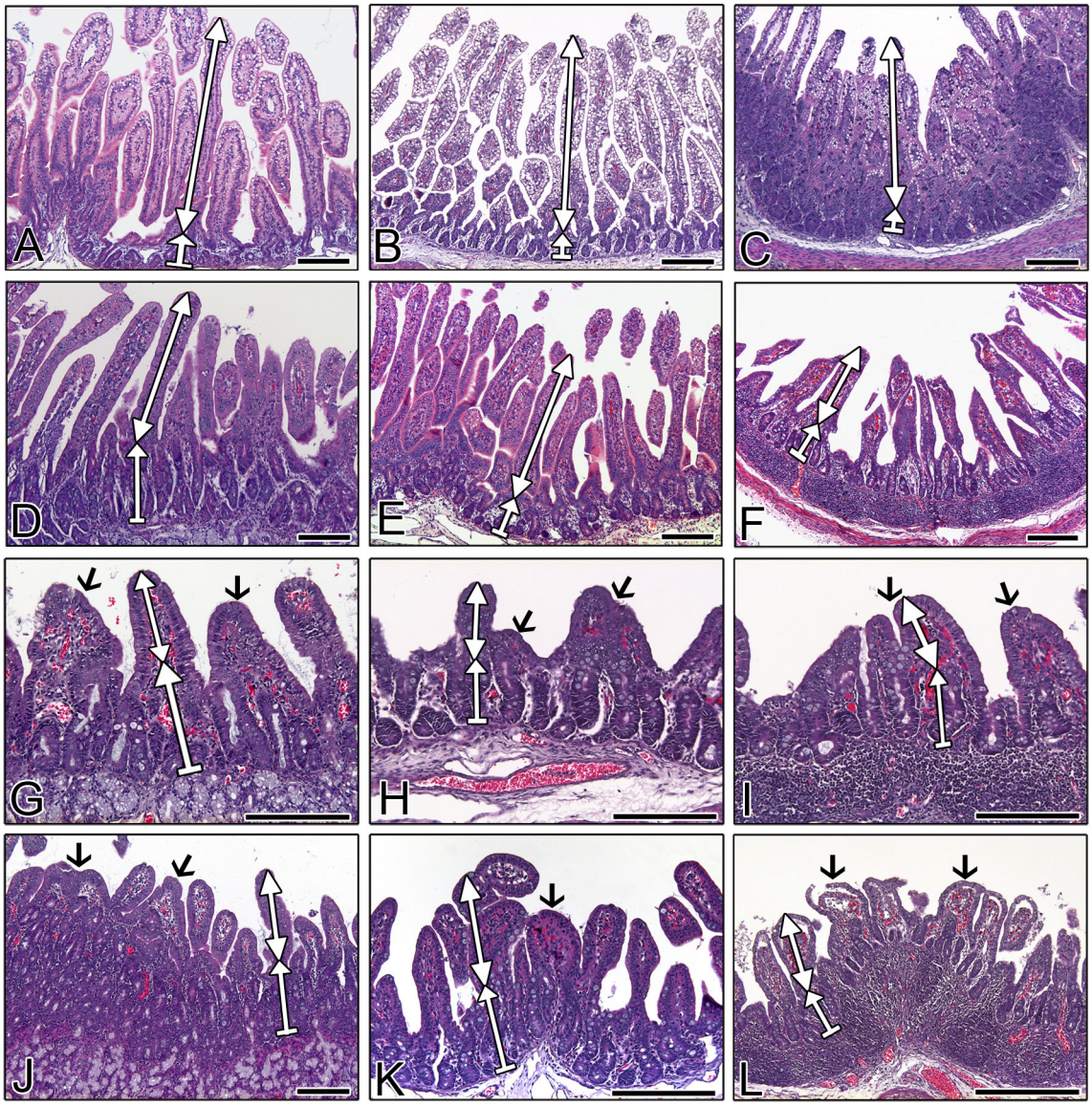

Fig. 1. Histopathological changes in the small intestine of piglets inoculated with PRG942 (G9P[23]) strain. Duodenum (A), jejunum (B), and ileum (C) from a mock-inoculated piglet had normal structure of mucosal membrane. Duodenum (D), jejunum (E), and ileum (F) sampled from a piglet inoculated with PRG942 (G9P[23]) strain at DPI 1 showed mild to moderate mucosal changes. Duodenum (G), jejunum (H), and ileum (I) sampled from a piglet inoculated with PRG942 (G9P[23]) strain at DPI 3 showed marked mucosal changes including the widespread villous atrophy (up-down arrow) and fusion (arrows), and increased crypt depth (up-wards arrow). Duodenum (J), jejunum (K), and ileum (L) sampled from a piglet inoculated with PRG942 (G9P[23]) strain at DPI 7 had marked mucosal changes. Samples were stained with hematoxylin and eosin stain. Bars A–L = 200 μm.

the RVA antigen distribution in intestines. Sequential changes of antigen distribution in the small intestines of piglets are summarized in Tables 3 and 4. Antigen-positive cells were detected in the villous epithelium and lymphoid cells in the lamina propria at DPI 1, and the number of positive-cells increased at DPI 3 but subsequently decreased from DPI 5 (Fig. 3, Tables 3 and 4). During the initial infection period from DPI 1 to DPI 3, antigen positive cells were detected equally in the villi epithelium and lymphoid cells in the lamina propria. As time elapsed, antigen positive cells were preferentially detected in the lymphoid cells due to increased desquamation of villi epithelium. No antigen-positive cells were observed in the small intestines sampled from either inactivated virus- or mock-inoculated piglets (Fig. 3, Tables 3 and 4).

3.4. Histological changes and RVA antigen localization in extra-intestinal organs and tissues

To evaluate the sequential changes of histopathological and antigen distribution in the extra-intestinal organs and tissues, samples were taken from piglets inoculated with PRG942 (G9P[23]) or PRG9121 (G9P[7]) at various times post inoculation. Sequential changes of antigen-positive

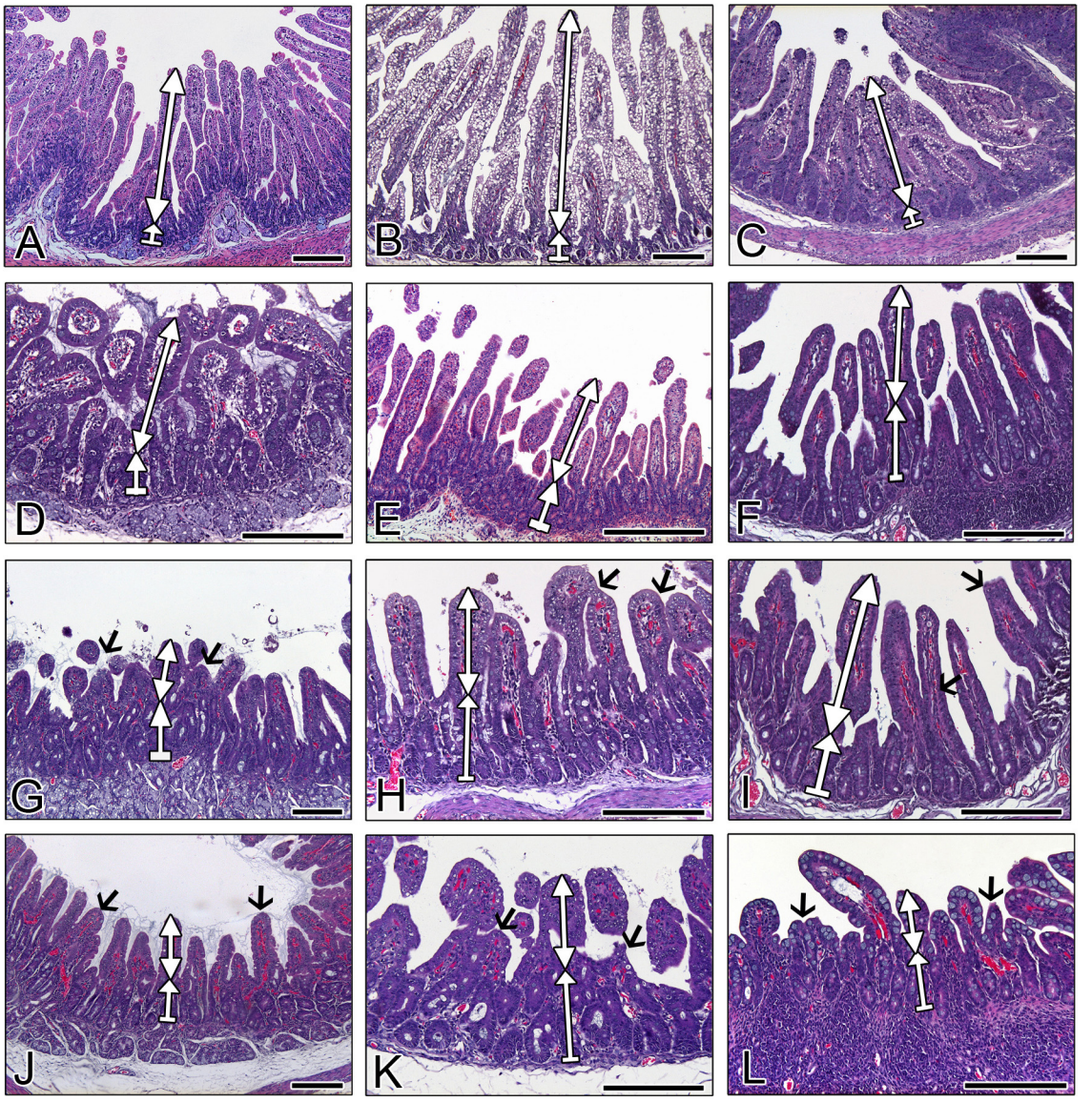

Fig. 2. Histopathological changes in the small intestine of piglets inoculated with PRG9121 (G9P[7]) strain. Duodenum (A), jejunum (B), and ileum (C) from a mock-infected piglet had normal structure of mucosal membrane. Duodenum (D), jejunum (E), and ileum (F) sampled from a piglet infected by PRG9121 (G9P[7]) strain at DPI 1 showed mild to moderate mucosal changes. Duodenum (G), jejunum (H), and ileum (I) sampled from a piglet inoculated with PRG9121 (G9P[7]) strain at DPI 3 showed marked mucosal changes including the widespread villous atrophy (up-down arrow) and fusion (arrows), and increased crypt depth (up-wards arrow). Duodenum (J), jejunum (K), and ileum (L) sampled from a piglet inoculated with PRG9121 (G9P[7]) strain at DPI 7 had marked mucosal changes. Samples were stained with hematoxylin and eosin stain. Bars A–L = 200 μm.

cells in the MLN, liver, lung and choroid plexus are summarized in Tables 5 and 6.

No histopathological changes and antigen-positive cells were observed in MLNs sampled from either inactivated virus- or mock-inoculated piglets (Figs. 4A and 5A). MLNs sampled from piglets inoculated with PRG942 (G9P[23]) or PRG9121(G9P[7]) showed lymphoid cell depletions and infiltration of macrophages and neutrophils in the cortex at DPI 3 (Figs. 4B and 5B). RVA-positive lymphoid cells were also detected in the MLNs at DPI 1, and their frequency increased to DPI 3 before gradually decreasing from DPI 5 (Figs. 4C and 5C, Tables 5 and 6).

Normal thin alveolar walls were observed in lungs sampled from inactivated virus- or mock-inoculated piglets (Figs. 4D and 5D). In contrast, the lung tissues sampled at DPI 3 displayed multiple interstitial thickenings due to hyperplasia of type II pneumocytes and infiltration of macrophages and lymphocytes with some neutrophils into the alveolar interstitium (Figs. 4E and 5E). RVA antigen was detected in a few pneumocytes and lymphoid cells in the lungs from piglets inoculated with PRG942 (G9P[23]) or PRG9121 (G9P[7]) strains from DPI 3 to DPI 7, but not from either inactivated virus- or mock-inoculated piglets (Figs. 4F and 5F, Tables 5 and 6).

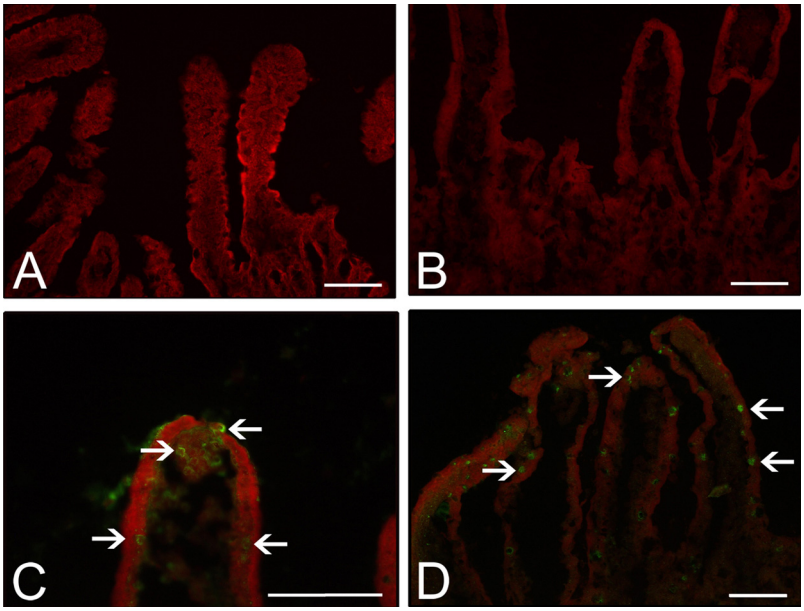

Fig. 3. Distribution of RVA-positive cells of PRG942 (G9P[23]) and PRG9121 (G9P[7]) strains in the duodenum. Piglets inoculated with either chloroform-inactivated PRG942 (G9P[23]) strain (A) or PRG9121 (G9P[7]) strain (B) contained no RVA-positive cells in the villi of each duodenum. RVA-positive cells (arrows) were scattered in the villi of duodenum sampled from piglets inoculated with PRG942 (G9P[23]) strain (C) or PRG9121 (G9P[7]) strain (D) at DPI 3. Indirect immunofluorescence assay was performed with monoclonal antibody against the VP6 protein of strain OSU. Bars A–D = 100 μm.

Normal liver sampled from inactivated virus- or mock-inoculated piglets showed intact hepatocytes (Figs. 4G and 5G), whereas degenerative or necrotic hepatocytes were observed in the livers sampled from virus-infected piglets (Figs. 4H and 5H). Some inflammatory cells including macrophages and lymphocytes were also observed in the livers sampled from virus-inoculated piglets. RVA antigen was detected in a few hepatocytes from DPI 3 to DPI 7 in

Table 5
The antigen distribution in the extra-intestinal organs of piglets inoculated with PRG942 (G9P[23]) strain.

Piglet No.	Inoculum	DPI at euthanasia	Distribution of RVA antigen in extra-intestinal organs[a]			
			Mesenteric lymph node	Liver	Lung	Choroid plexus
1	PRG942	1	2.6	0	0	0
2	PRG942	1	2.2	0	0	0
3	PRG942	3	3.2	1.2	0.4	0.4
4	PRG942	3	3.4	1.6	0.6	0.6
5	PRG942	5	2.4	1.6	0.4	0.2
6	PRG942	7	1.6	1	0.2	0.2
7	PRG942	14	1.2	0	0	0
8	Mock	2	0	0	0	0
9	Inactivated PRG942	3	0	0	0	0

[a] The antigen distribution in the extra-intestinal organs was evaluated based on the number of antigen-positive, and was measured as follows: 0 = no positive cells, 1 = one to two positive cells, 2 = three to five positive cells scattered in tissue, 3 = many positive cells in tissues, 4 = positive in most tissue.

Table 6
The antigen distribution in the extra-intestinal organs of piglets inoculated with PRG9121 (G9P[7]) strain.

Piglet No.	Inoculum	DPI at euthanasia	Distribution of RVA antigen in extra-intestinal organs[a]			
			Mesenteric lymph node	Liver	Lung	Choroid plexus
1	PRG9121	1	2	0	0	0
2	PRG9121	1	1.8	0	0	0
3	PRG9121	3	3.6	1	0.6	0.2
4	PRG9121	3	3.4	1.4	0.6	0.4
5	PRG9121	5	2	1	0.2	0.4
6	PRG9121	7	1	0.2	0.2	0.4
7	PRG9121	14	0.4	0	0	0
8	Mock	2	0	0	0	0
9	Inactivated PRG9121	3	0	0	0	0

[a] The antigen distribution in the extra-intestinal organs was evaluated based on the number of antigen-positive, and was measured as follows: 0 = no positive cells, 1 = one to two positive cells, 2 = three to five positive cells scattered in tissue, 3 = many positive cells in tissues, 4 = positive in most tissue.

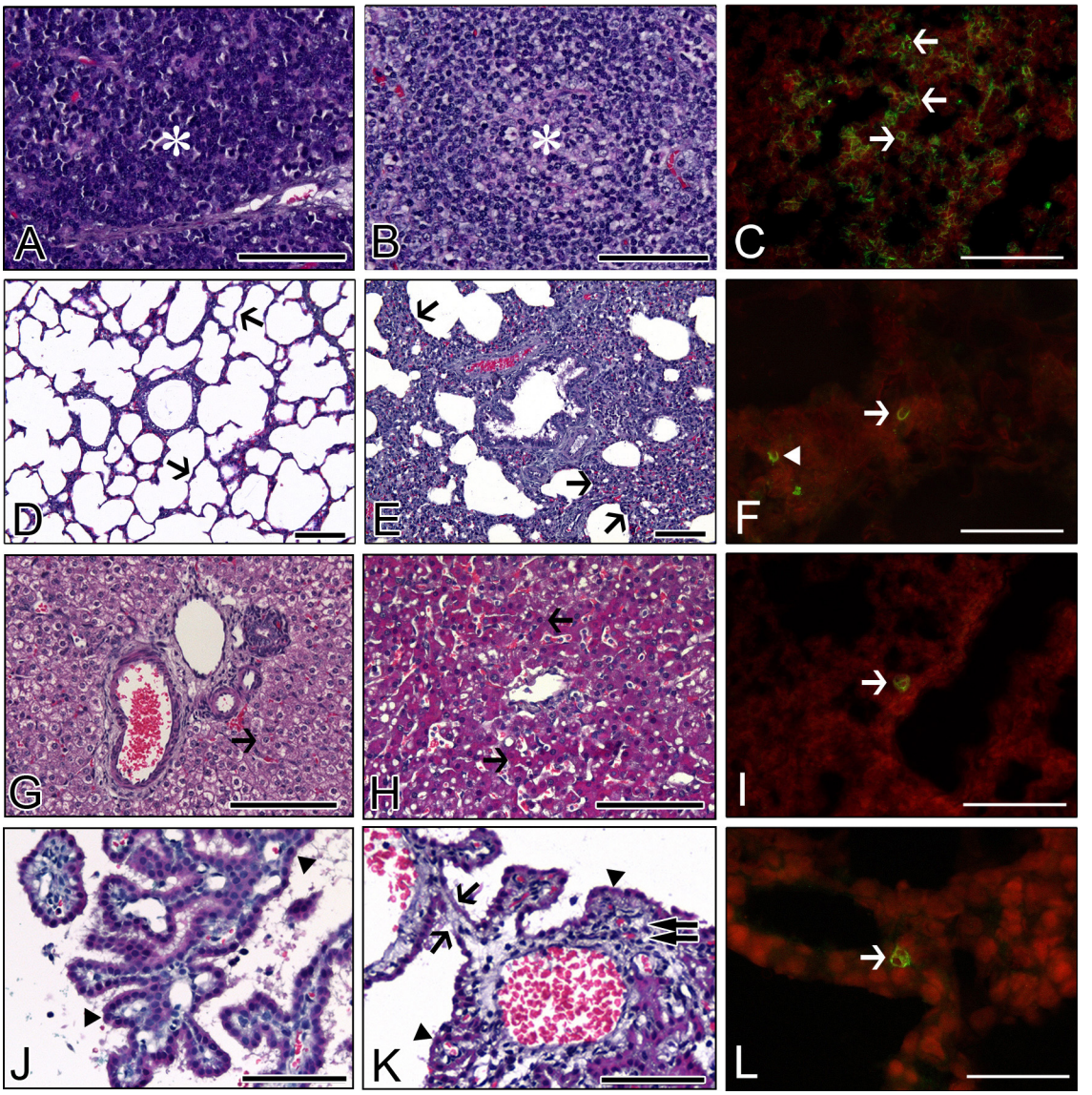

Fig. 4. Histopathological findings and antigen distribution in the extra-intestinal organs of piglets inoculated with PRG942 (G9P[23]) strain. (A) Normal mesenteric lymph node (MLN) sampled from a mock-inoculated piglet showed intact cortex with densely concentrated lymphocytes (asterisk). (B) MLN sampled from a piglet inoculated with PRG942 (G9P[23]) strain at DPI 3 showed lymphoid cell depletion in the cortex (asterisk). (C) RVA-positive lymphoid cells (arrows) were scattered in the MLN from a piglet inoculated with PRG942 (G9P[23]) strain at DPI 3. (D) Normal lung tissue sampled from a mock-inoculated piglet had thin alveolar walls (arrows). (E) Lung tissue sampled from a piglet inoculated with PRG942 (G9P[23]) strain at DPI 3 showed interstitial pneumonia (arrows). (F) RVA antigens were detected in a pneumocyte (arrowhead) and lymphoid cell (arrow) in the lung from a piglet inoculated with PRG942 (G9P[23]) strain at DPI 3. (G) Normal liver sampled from a mock-inoculated piglet showed fat-stored hepatocytes (arrow). (H) Multiple necrotic hepatocytes scattered in the liver sampled from a piglet inoculated with PRG942 (G9P[23]) strain at DPI 3 showed pyknosis of nucleus and increased eosinophilia of cytoplasm (arrows). (I) RVA antigens were detected in a hepatocyte (arrow) in the liver from a piglet inoculated with PRG942 (G9P[23]) strain at DPI 3. (J) Intact epithelium (arrowheads) was observed in the choroid plexus sampled from a mock-inoculated piglet. (K) Choroid plexus sampled from a piglet inoculated with PRG942 (G9P[23]) strain at DPI 3 showed epithelial degeneration (arrowheads), necrosis (arrows), and lymphocyte infiltration (double arrows). (L) RVA antigens were detected in the epithelial cells (arrow) of the choroid plexus from a piglet inoculated with PRG942 (G9P[23]) strain at DPI 3. Bars A–L = 100 μm.

the livers from piglets inoculated with each strain, but not from either inactivated virus- or mock-inoculated piglets (Figs. 4I and 5I, Tables 5 and 6).

An intact epithelium was observed in the choroid plexus sampled from inactivated virus- or mock-inoculated piglets (Figs. 4J and 5J). In contrast, choroid plexus sampled from piglets inoculated with PRG942 (G9P[23]) or PRG9121 (G9P[7]) displayed epithelial degeneration and necrosis. In addition, some lymphocytes were observed infiltrating into the tela choroidea (Figs. 4K and 5K). RVA antigen was detected in a few epithelial cells and lymphoid cells from DPI 3 to DPI 7 in the choroid plexus from piglets inoculated with both strains, but not from either inactivated virus- or mock-inoculated piglets (Figs. 4L and 5L, Tables 5 and 6).

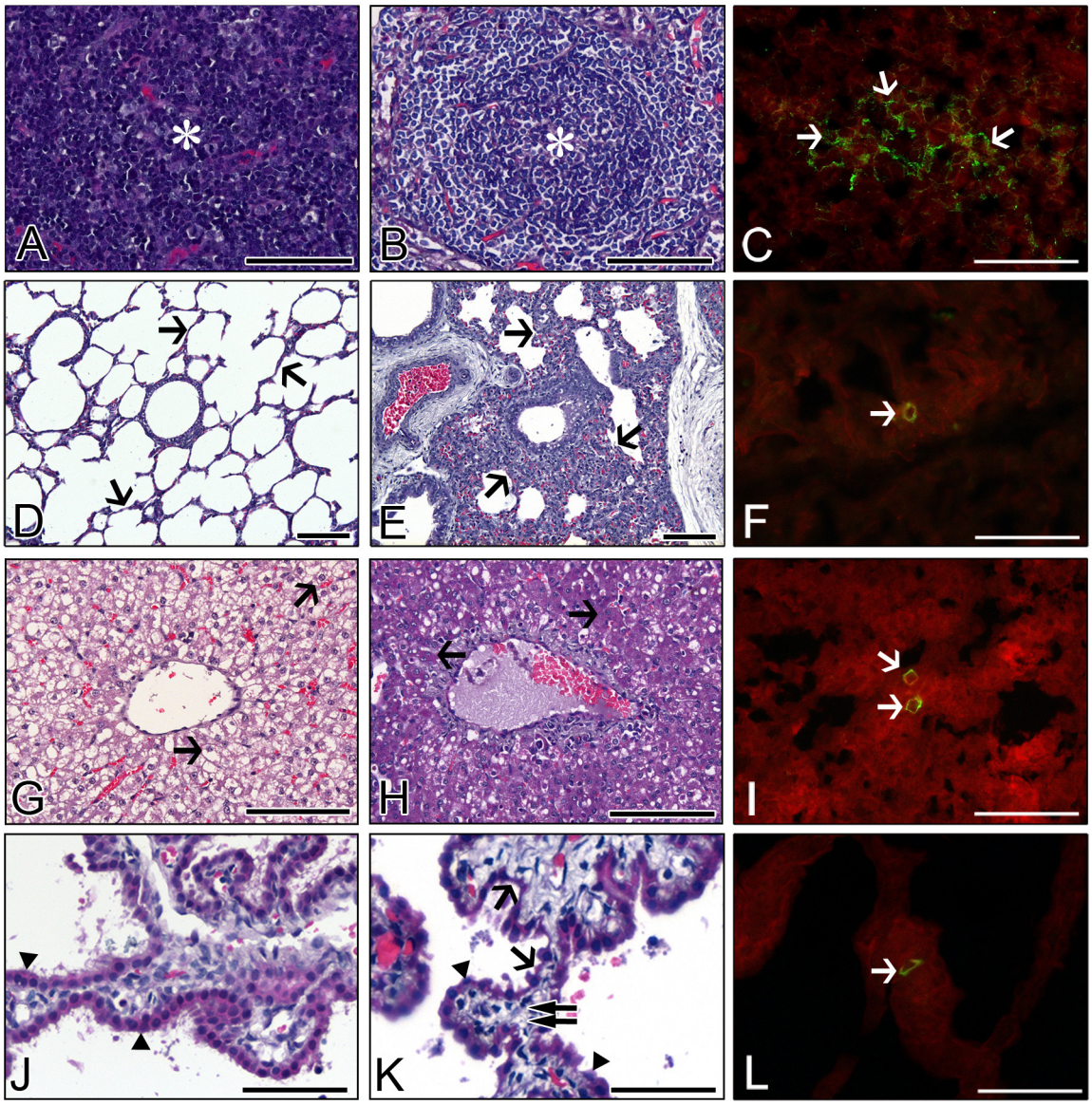

Fig. 5. Histopathological findings and antigen distribution in the extra-intestinal organs of piglets inoculated with PRG9121 (G9P[7]) strain. (A) Normal mesenteric lymph node (MLN) sampled from a mock-inoculated piglet showed intact cortex with densely concentrated lymphocytes (asterisk). (B) MLN sampled from a piglet inoculated with PRG9121 (G9P[7]) strain at DPI 3 showed marked lymphoid cell depletion in the cortex (asterisk). (C) RVA-positive lymphoid cells (arrows) were scattered in the MLN from a piglet inoculated with PRG9121 (G9P[7]) strain at DPI 3. (D) Normal lung tissues sampled from a mock-inoculated piglet had thin alveolar walls (arrows). (E) Lung tissues sampled from a piglet inoculated with PRG9121 (G9P[7]) strain at DPI 3 showed interstitial pneumonia (arrows). (F) RVA antigen was detected in a pneumocyte (arrow) in the lung from a piglet inoculated with PRG9121 (G9P[7]) strain at DPI 3. (G) Normal liver sampled from a mock-inoculated piglet showed fat-stored hepatocytes (arrows). (H) Multiple necrotic hepatocytes scattered in the liver sampled from a piglet inoculated with PRG942 (G9P[23]) strain at DPI 3 showed pyknosis of nucleus and increased eosinophilia of cytoplasm (arrows). (I) RVA antigens were detected in a few hepatocytes (arrows) in the liver from a piglet inoculated with PRG9121 (G9P[7]) strain at DPI 3. (J) Intact epithelium (arrowheads) was observed in the choroid plexus sampled from a mock-inoculated piglet. (K) Choroid plexus sampled from a piglet inoculated with PRG9121 (G9P[7]) strain at DPI 3 showed epithelial degeneration (arrowheads), necrosis (arrows), and lymphocyte infiltration (double arrows). (L) RVA antigen was detected in a lymphoid cell (arrow) in the choroid plexus from a piglet inoculated with PRG9121 (G9P[7]) strain. Bars A–L = 100 μm.

3.5. Quantification of RVA RNA in the feces, nasal swabs, blood, and extra-intestinal organs and tissues

SYBR Green real-time RT-PCR assays were performed to evaluate the viral RNA copy numbers in the feces, blood, MLN, liver, lung, choroid plexus, and nasal swab sampled from G9 RVA-inoculated piglets. As expected, viral RNA was not detected in these specimens sampled from either inactivated virus- or mock-inoculated piglets.

High viral loads of 6.3×10^4/mg and 5.0×10^4/mg feces were detected in fecal samples at DPI 1 before reaching a peak at DPI 3 (7.3×10^6/mg and 9.8×10^5/mg feces), and then gradually decreased from DPI 5 to 14 in the G9P[23] PRG942-inoculated or G9P[7] PRG9121-inoculated piglets,

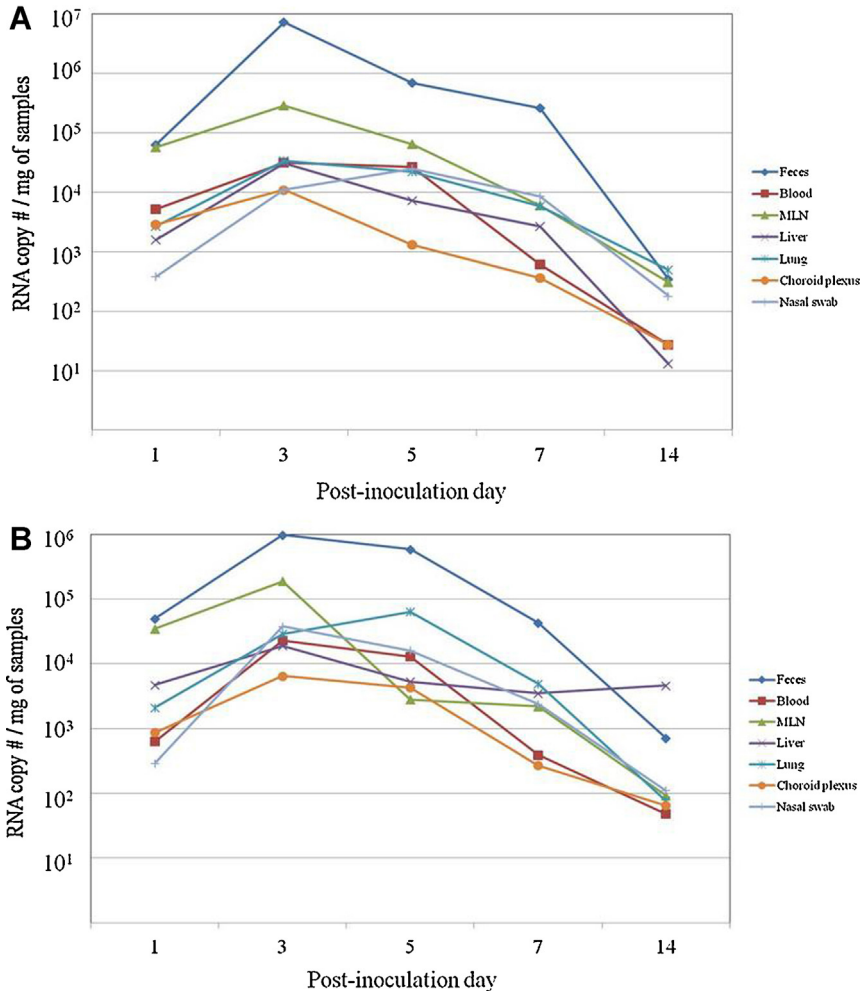

Fig. 6. Quantification of RVA RNA by SYBR Green real-time RT-PCR. Real-time RT-PCR was performed with the feces, serum, mesenteric lymph node (MLN), liver, lung, choroid plexus, and nasal swab sampled from piglets inoculated with porcine G9 RVA strain PRG942 (G9P[23]) (A) and PRG9121 (G9P[7]) (B). The geometric means of viral RNA copy number per mg of tissue are displayed.

respectively (Fig. 6A and B). In blood samples, viral RNAs were detected at DPI 1 (5.2×10^3/mg and 6.3×10^2/mg serum), reached a peak at DPI 3 (3.2×10^4/mg and 2.3×10^4/mg serum), and then rapidly declined after DPI 5 in the G9P[23] PRG942-inoculated or G9P[7] PRG9121-inoculated piglets, respectively (Fig. 6A and B).

Among the extra-intestinal organs and tissues sampled, the highest viral RNA copy numbers were observed in the MLN from piglets inoculated with PRG942 (G9P[23]) or PRG9121 (G9P[7]). Viral RNA was detected in the MLNs at DPI 1 (5.7×10^4/mg and 3.5×10^4/mg tissue, same respective order), reaching a peak at DPI 3 (2.9×10^5/mg and 1.9×10^5/mg tissue, same respective order), and rapidly decreasing after DPI 3 (Fig. 6A and B).

Viral RNA was detected at DPI 1 (1.6×10^3/mg tissue) in the liver of piglet infected with G9P[23] PRG942 strain, reaching a peak at DPI 3 (3.1×10^4/mg tissue) before continuously decreasing to 1.3×10^1/mg tissue at DPI 14 (Fig. 6A). In contrast, viral RNA was detected at DPI 1 (4.7×10^3/mg tissue) in the liver from piglets infected with G9P[7] PRG9121 strain, also reaching a peak at DPI 3 (1.9×10^4/mg tissue) and further persisting around 3.5–5.3×10^3/mg tissue from DPI 5 to 14 (Fig. 6B).

In the lung samples, viral RNA was detected at DPI 1 (2.7×10^3/mg tissue) from piglets infected with PRG942 (G9P[23]) strain, reaching a peak at DPI 3 (3.4×10^4/mg tissue) and gradually decreasing until DPI 14 (Fig. 6A). In contrast, viral RNA was detected at DPI 1 (2.1×10^3/mg tissue) in the lung from piglets infected with PRG9121 (G9P[7]) strain, reaching a peak at DPI 5 (6.4×10^4/mg tissue), after which the copy number rapidly decreased (Fig. 6B).

In the choroid plexus, viral RNAs were also detected at DPI 1 (2.9×10^3/mg and 8.7×10^2/mg tissue), reaching a peak at DPI 3 (1.1×10^4/mg and 6.5×10^3/mg tissue) and then decreasing gradually after DPI 3 in piglets inoculated with either the PRG942 (G9P[23]) or PRG9121 (G9P[7]) strain (Fig. 6A and B).

Viral RNA in the nasal swab from piglet inoculated with PRG942 (G9P[23]) strain was detected at DPI 1 (3.8×10^2/

mg fluid), reaching a peak at DPI 5 (2.5×10^4/mg fluid) and gradually decreased after DPI 5 (Fig. 6A). In contrast, viral RNA from piglet inoculated with PRG9121 (G9P[7]) strain was detected at DPI 1 (2.9×10^2/mg fluid), peaked at DPI 3 (3.8×10^4/mg fluid), then gradually decreased until DPI 14 (Fig. 6B).

4. Discussion

RVA can infect and cause clinical disease in humans and a wide range of animal species (Estes and Kapikian, 2007). As a common disease in humans and animals, transmission of RVA from one species to another may occur and leads to public health concerns, particularly in developing countries, where humans and animals often live in close proximity and mixed infections are rather common (Jain et al., 2001; Leite et al., 1996; Timenetsky et al., 1994; Unicomb et al., 1999). To date, the G9 RVA strains have only been detected in humans and pigs, and pigs are hypothesized to be a potential reservoir for human G9 RVAs (Collins et al., 2010; Mascarenhas et al., 2007; Matthijnssens et al., 2010a). G9 RVAs can be classified phylogenetically into I-VI lineages, with lineage I-II consisting of strains isolated in the 1980s, and III-VI composing of strains isolated from the mid-1990s (Phan et al., 2007). Of these, lineages III and VI were found in both humans and pigs (Phan et al., 2007). Interestingly, human lineage 3 G9 RVA strains were previously shown to be both phylogentically and antigenically related to the first described porcine G9 RVA strain A2 (Hoshino et al., 2005). Both porcine G9 RVA strains used in this study clustered in lineage VI of known porcine and human G9 RVAs. Moreover, these strains possessed the following porcine/human Wa-like genotypes: R1–C1–M1–N1–T1–E1–H1 plus porcine specific genotypes P[7]/P[23]-I5-A8 (Kim et al., 2012a). However, these porcine specific genotypes have been detected in humans and other species as well, most likely as a result of interspecies transmission (Ghosh et al., 2012; Varghese et al., 2004; Zeller et al., 2012). In addition, the human reference strain Wa replicates in experimental pigs, resulting in diarrhea and intestinal pathology (Azevedo et al., 2005). These findings may indicate that G9 RVAs with a (partially) Wa-like genotype constellation are capable to cause successful interspecies transmissions at least between humans and pigs. Therefore, it is important to determine whether G9 bearing RVAs can induce typical RVA-associated disease in animal models. In the present study, we have demonstrated that both porcine G9 RVA strains induced typical RVA-associated disease, including diarrhea, histopathological changes in intestinal and extra-intestinal organs or tissues, and viremia in experimentally infected piglets. Our results provide a new perspective on the pathogenesis of G9 RVAs in a pig model, confirming that like other human and animal RVAs, intestinal and extra-intestinal tropisms and viremia can be induced in an animal RVA disease model. To our knowledge, this study is the first to describe the intestinal and extra-intestinal pathogenicity of G9 bearing RVAs in an experimental pig model. Our data will also contribute to increased understanding of infection, pathology, disease, immunity, and testing of prospective vaccines and drugs against both human and animal G9 RVAs.

The degree of diarrhea and intestinal pathological changes by RVA infection vary among animal species (Boshuizen et al., 2003; Lundgren and Svensson, 2001; Ramig, 2004; Shepherd et al., 1979; Snodgrass et al., 1979). In the present study, both porcine G9P[23]/P[7] strains induced diarrhea at DPI 1 in colostrum-deprived piglets, which lasted to DPI 8. Moreover, these strains induced almost similar histopathological small intestinal lesion changes; mild villous atrophy and crypt hyperplasia at DPI 1 became marked from DPI 5 and persisted to DPI 14. Replication of both G9 strains occurred most efficiently in the intestine because the viral RNA copy numbers in the fecal samples were ~25-fold greater than that seen in the next most prominent site, the MLN, and ~660-fold greater than that found in other organs at DPI 3. It has also been shown that the number of antigen positive cells was the highest in the small intestinal villi. In addition, the high intestinal lesion scores at DPI 14 (after the disappearance of diarrhea) were due to sustained strong crypt hyperplasia, resulting in low villi versus crypt ratios. It is important to note that, since the intestinal samples were taken from only one or two experimental piglets sacrificed on any given day, further studies will be needed to increase the number of experimental piglets to obtain more robust statistical data. However, overall these combined data indicate that both G9P[23]/P[7] strains display a strong intestinal tropism and virulence in piglets.

Previous findings suggested that rotaviral antigenemia is common in humans and animals, and can occur during both homologous and heterologous RVA infections (Blutt et al., 2003; Chiappini et al., 2005; Fenaux et al., 2006; Fischer et al., 2005; Li and Wang, 2003; Mossel and Ramig, 2003; Zhao et al., 2005). Moreover, some studies revealed the presence of RVA RNA in the sera of infants, primates, and swine during acute infection (Azevedo et al., 2005; Blutt et al., 2003; Chiappini et al., 2005; Fenaux et al., 2006; Fischer et al., 2005; Kim et al., 2011, 2012b; Li and Wang, 2003; Zhao et al., 2005). It has been suggested that denudation of villi due to acute and severe destruction of overlaying enterocytes could be the major route for cell-free virus entrance to the blood circulation and subsequent spread to extra-intestinal organs and tissues (Azevedo et al., 2005; Fenaux et al., 2006; Kim et al., 2011, 2012b). This hypothesis is consistent with the present results as viral RNA loads were detected by real-time RT-PCR in the cell-free sera at DPI 1, reaching a peak at DPI 3 or 5, and then gradually decreasing but persisting up to DPI 14.

Another possible route for RVA entrance to the bloodstream is cell-associated viremia transmission (Brown and Offit, 1998; Dharakul et al., 1988). The ability of RVA to infect certain lymphocyte subsets or to be taken by antigen-presenting cells in the gut-associated lymphoid tissue could indicate a potential route of viral spread from the intestine to other organs (Fenaux et al., 2006). In the present study, antigen-positive lymphoid cells were detected in the lamina propria of the villi in the piglets infected with either G9P[23] or G9P[7], supporting the role of cell-associated viremia. Moreover, MLNs were shown to be the second most susceptible tissues with high antigen

and viral RNA loads in the lymphoid cells of animals infected with both strains throughout the experiment. Histopathologically, MLNs showed lymphoid cell necrosis and deficiency, resulting from RVA replication. Therefore, it could be argued that MLNs act as a secondary amplifier and a portal of systemic entry through either the lymphatic network or the blood (Brown and Offit, 1998; Fenaux et al., 2006; Mossel and Ramig, 2003). In addition, it was reported that cell-free viremia rather than cell-associated viremia via the bloodstream seems to be major path of viral spread in a mouse model (Fenaux et al., 2006). At this stage however, it is important to note that we cannot determine whether RVA antigens detected in the lymphoid cells were due to authentic RVA replication in the lymphoid cells or simply represent antigen taken up by the B lymphocytes to process the antigen. As an additional minor point of caution, it should be noted that the pathological, virological, and immunological events of RVA infections in the porcine and mouse models may be different and could also be distinct from what occurs in humans.

Initially, RVA infections were thought to be restricted to small intestine (Blutt and Conner, 2007). However, there is now growing evidence that extra-intestinal replication and lesions associated with RVA infections can occur in humans and animals (Blutt et al., 2003: Ciarlet et al., 2002; Crawford et al., 2006; Fenaux et al., 2006). As mentioned above, both G9P[23] and G9P[7] RVA strains caused small intestinal pathology and viremia in the experimental piglets, which can mediate RVA spread to extra-intestinal organs or tissues. Therefore, we assessed where and when RVA antigen and RNA was present outside the small intestine and how many viral RNA copies could be found at various sites. Antigen-positive cells of both strains were detected in many more cells of the MLN than those of the liver, lung, and choroid plexus. The viral RNA loads also reached a peak during this period, which was 0 to 3 logs lower than the viral load in MLN and feces. From these findings, it could be concluded that porcine G9 RVA can replicate, albeit to a limited extent, in the extra-intestinal organs including the MLN, liver, lung, and choroid plexus. These results are consistent with other studies that indicate the ability of G9 RVA virions to spread to the blood and to substantially extend to the extra-intestinal organs (Blutt et al., 2003; Ciarlet et al., 2002; Crawford et al., 2006; Fenaux et al., 2006; Kim et al., 2011). In addition, our results indicated that although porcine G9 strains infected and replicated in the extra-intestinal organs or tissues, the severity of RVA-associated lesions in these organs and tissues was lesser than that of small intestine and MLN.

It should be noted that these RVA-associated lesions in these extra-intestinal organs and tissues can induce more serious diseases when complicated with other pathogens or diseases. For example, many viral pathogens such as influenza virus, porcine reproductive and respiratory syndrome virus, porcine respiratory coronavirus and porcine circovirus type 2 play crucial role as a primary pathogen for developing porcine respiratory disease complex (PRDC), which is one of the most important diseases in the pig industry (Brockmeier et al., 2002). These viral pathogens injure the ciliated or pulmonary epithelium of the respiratory tract, cause damage to the function of pulmonary macrophages, and alter immunomodulatory effects. The suppressed defense mechanisms of the respiratory tract facilitate secondary bacterial infection with *Mycoplasma hyopneumoniae*, *Actinobacillus pleuropneumoniae*, and *Pasteurella mutocida*, resulting in PRDC. In this study, both RVA strains injured alveolar epithelium, resulting in interstitial pneumonia. Thus, it can be speculated that RVA can act as a primary pathogen to alter the defense mechanisms of the respiratory tract, to facilitate the secondary bacterial infection and finally to evoke PRDC. Further study should address whether RVA infection can induce PRDC when complicated with secondary bacterial infection.

In conclusion, the porcine G9 bearing RVA strains display a strong tropism for the small intestine and are virulent in experimentally infected piglets. Both porcine G9 RVA strains share the ability to escape the small intestine, spread systemically via viremia, and replicate in extra-intestinal organs and tissues. Our data indicate that MLNs may play a critical role in RVA escape from the small intestine by providing a site for substantial and prolonged secondary viral replication before extending to extra-intestinal organs and tissues. A detailed understanding of the mechanisms that determine intestinal and extra-intestinal pathogenicity, combined with the availability of effective preventive and therapeutic measures, is critical for the control of RVA infection. However, to date, animal models to understand pathogenesis of porcine and human G9 RVAs have not established. Therefore, we expect that the present results could contribute to our understanding of the pathogenesis of human G9 RVAs, and pig model with porcine G9 strains could be suitable for evaluating not only the efficacy of vaccines but also anti-viral drug candidates of both these important pathogens.

Acknowledgments

This study was supported by the National Research Foundation grant funded by the Korea Government (MEST) (No. 2010-0002047), Republic of Korea. The authors acknowledge a graduate fellowship provided by the Korean Ministry of Science, ICT and Future Planning through the Brain Korea 21 Plus project. We thank Dr. Ian Goodfellow for critical reading of this manuscript. J.M was supported by an FWO ('Fonds voor Wetenschappelijk Onderzoek') post-doctoral fellowship.

References

Azevedo, A.S., Yuan, L., Jeong, K.I., González, A., Nguyen, T.V., Pouly, S., Gochnauer, M., Zhang, W., Azevedo, A., Saif, L.J., 2005. Viremia and nasal and rectal shedding of rotavirus in gnotobiotic pigs inoculated with Wa human rotavirus. J. Virol. 79, 5428–5436.

Barril, P.A., Martinez, L.C., Giordano, M.O., Castello, A.A., Rota, R.P., Isa, M.B., Masachessi, G., Ferreyra, L.J., Glikmann, G., Nates, S.V., 2006. Detection of group a human rotavirus G9 genotype circulating in Córdoba, Argentina, as early as 1980. J. Med. Virol. 78, 1113–1118.

Blutt, S.E., Conner, M.E., 2007. Rotavirus: to the gut and beyond! Curr. Opin. Gastroenterol. 23, 39–43.

Blutt, S.E., Kirkwood, C.D., Parreño, V., Warfield, K.L., Ciarlet, M., Estes, M.K., Bok, K., Bishop, R.F., Conner, M.E., 2003. Rotavirus antigenaemia and viraemia: a common event? Lancet 362, 1445–1449.

Boshuizen, J.A., Reimerink, J.H., Korteland-van Male, A.M., van Ham, V.J., Koopmans, M.P., Büller, H.A., Dekker, J., Einerhand, A.W., 2003. Changes in small intestinal homeostasis, morphology, and gene expression during rotavirus infection of infant mice. J. Virol. 77, 13005–13016.

Brockmeier, S.L., Halbur, P.G., Thacker, E.L., 2002. Porcine respiratory disease complex. In: Brogden, K.A., Guthmiller, J.M. (Eds.), Polymicrobial Diseases. ASM Press, Washington, DC, pp. 231–258.

Brown, K.A., Offit, P.A., 1998. Rotavirus-specific proteins are detected in murine macrophages in both intestinal and extra intestinal lymphoid tissues. Microb. Pathog. 24, 327–331.

Cao, D., Santos, N., Jones, R.W., Tatsumi, M., Gentsch, J.R., Hoshino, Y., 2008. The VP7 genes of two G9 rotaviruses isolated in 1980 from diarrheal stool samples collected in Washington, DC, are unique molecularly and serotypically. J. Virol. 82, 4175–4179.

Chiappini, E., Azzari, C., Moriondo, M., Galli, L., de Martino, M., 2005. Viraemia is a common finding in immunocompetent children with rotavirus infection. J. Med. Virol. 76, 265–267.

Ciarlet, M., Conner, M.E., Finegold, M.J., Estes, M.K., 2002. Group A rotavirus infection and age-dependent diarrheal disease in rats: a new animal model to study the pathophysiology of rotavirus infection. J. Virol. 76, 41–57.

Collins, P.J., Martella, V., Sleator, R.D., Fanning, S., O'Shea, H., 2010. Detection and characterisation of group A rotavirus in asymptomatic piglets in southern Ireland. Arch. Virol. 155, 1247–1259.

Crawford, S.E., Patel, D.G., Cheng, E., Berkova, Z., Hyser, J.M., Ciarlet, M., Finegold, M.J., Conner, M.E., Estes, M.K., 2006. Rotavirus viremia and extra intestinal viral infection in the neonatal rat model. J. Virol. 80, 4820–4832.

Dharakul, T., Riepenhoff-Talty, M., Albini, B., Ogra, P.L., 1988. Distribution of rotavirus antigen in intestinal lymphoid tissues: potential role in development of the mucosal immune response to rotavirus. Clin. Exp. Immunol. 74, 14–19.

Estes, M.K., Kapikian, A.Z., 2007. Rotaviruses. In: Knipe, D.M., Griffin, D.E., Lamb, R.A., Straus, S.E., Howley, P.M., Martin, M.A., Roizman, B. (Eds.), Fields Virology. fifth ed. Lippincott Williams & Wilkins, Philadelphia, pp. 1917–1974.

Fenaux, M., Cuadras, M.A., Feng, N., Jaimes, M., Greenberg, H.B., 2006. Extraintestinal spread and replication of a homologous EC rotavirus strain and a heterologous Rhesus rotavirus in BALB/c mice. J. Virol. 80, 5219–5232.

Fischer, T.K., Ashely, D., Kerin, K., Reynolds-Hedmann, E., Gentsch, J., Widdowson, M.-A., Westerman, L., Ruhr, N., Turcios, R.M., Glass, R.I., 2005. Rotavirus antigenemia in patients with acute gastroenteritis. J. Infect. Dis. 192, 913–919.

Gentsch, J.R., Laird, A.R., Bielfelt, B., Griffin, D.D., Bányai, K., Ramachandran, M., Jain, V., Cunliffe, N.A., Nakagomi, O., Kirkwood, C.D., Fischer, T.K., Parashar, U.D., Bresee, J.S., Jiang, B., Glass, R.I., 2005. Serotype diversity and reassortment between human and animal rotavirus strains: implications for rotavirus vaccine programs. J. Infect. Dis. 192 (Suppl. 1) S146–S159.

Ghosh, S., Shintani, T., Kobayashi, N., 2012. Evidence for the porcine origin of equine rotavirus strain H-1. Vet. Microbiol. 158, 410–414.

Hoshino, Y., Honma, S., Jones, R.W., Ross, J., Santos, N., Gentsch, J.R., Kapikian, A.Z., Hesse, R.A., 2005. A porcine G9 rotavirus strain shares neutralization and VP7 phylogenetic sequence lineage 3 characteristics with contemporary human G9 rotavirus strains. Virology 332, 177–188.

Jain, V., Das, B.K., Bhan, M.K., Glass, R.I., Gentsch, J.R., 2001. Great diversity of group A rotavirus strains and high prevalence of mixed rotavirus infections in India. J. Clin. Microbiol. 39, 3524–3529.

Kim, H.H., Matthijnssens, J., Kim, H.J., Kwon, H.J., Park, J.G., Son, K.Y., Ryu, E.H., Kim, D.S., Lee, W.S., Kang, M.I., Yang, D.K., Hyun, B.H., Park, S.I., Park, S.J., Cho, K.O., 2012a. Full-length genomic analysis of porcine G9P[23] and G9P[7] rotavirus strains isolated from pigs with diarrhea in South Korea. Infect. Genet. Evol. 12, 1427–1435.

Kim, H.J., Park, J.G., Alfajaro, M.M., Kim, D.S., Hosmillo, M., Son, K.Y., Lee, J.H., Bae, Y.C., Park, S.I., Kang, M.I., Cho, K.O., 2012b. Pathogenicity characterization of a bovine triple reassortant rotavirus in calves and piglets. Vet. Microbiol. 159 (1–2) 11–22.

Kim, H.J., Park, J.G., Matthijnssens, J., Lee, J.H., Bae, Y.C., Alfajaro, M.M., Park, S.I., Kang, M.I., Cho, K.O., 2011. Intestinal and extra-intestinal pathogenicity of a bovine reassortant rotavirus in calves and piglets. Vet. Microbiol. 152, 291–303.

Kim, H.J., Park, S.I., Ha, T.P., Jeong, Y.J., Kim, H.H., Kwon, H.J., Kang, M.I., Cho, K.O., Park, S.J., 2010. Detection and genotyping of Korean porcine rotaviruses. Vet. Microbiol. 144, 274–286.

Leite, J.P., Alfieri, A.A., Woods, P.A., Glass, R.I., Gentsch, J.R., 1996. Rotavirus G and P types circulating in Brazil: characterization by RT-PCR, probe hybridization, and sequence analysis. Arch. Virol. 141, 2365–2374.

Li, N., Wang, Z.Y., 2003. Viremia and extraintestinal infections in infants with rotavirus diarrhea. Di Yi Jun Yi Da Xue Xue Bao 23, 643–648.

Lundgren, O., Svensson, L., 2001. Pathogenesis of rotavirus diarrhea. Microbes Infect. 3, 1145–1156.

Lynch, M., Lee, B., Azimi, P., Gentsch, J., Glaser, C., Gilliam, S., Chang, H.G., Ward, R., Glass, R.I., 2001. Rotavirus and central nervous system symptoms: cause or contaminant? Case reports and review. Clin. Infect. Dis. 33, 932–938.

Martella, V., Bányai, K., Matthijnssens, J., Buonavoglia, C., Ciarlet, M., 2010. Zoonotic aspects of rotaviruses. Vet. Microbiol. 140, 246–255.

Mascarenhas, J.D., Leite, J.P., Lima, J.C., Heinemann, M.B., Oliveira, D.S., Araújo, I.T., Soares, L.S., Gusmão, R.H., Gabbay, Y.B., Linhares, A.C., 2007. Detection of a neonatal human rotavirus strain with VP4 and NSP4 genes of porcine origin. J. Med. Microbiol. 56, 524–532.

Matthijnssens, J., Ciarlet, M., Heiman, E., Arijs, I., Delbeke, T., McDonald, S.M., Palombo, E.A., Iturriza-Gómara, M., Maes, P., Patton, J.T., Rahman, M., Van Ranst, M., 2008a. Full genome-based classification of rotaviruses reveals a common origin between human Wa-like and porcine rotavirus strains and human DS-1-like and bovine rotavirus strains. J. Virol. 82, 3204–3219.

Matthijnssens, J., Ciarlet, M., Rahman, M., Attoui, H., Bányai, K., Estes, M.K., Gentsch, J.R., Iturriza-Gómara, M., Kirkwood, C.D., Martella, V., Mertens, P.P., Nakagomi, O., Patton, J.T., Ruggeri, F.M., Saif, L.J., Santos, N., Steyer, A., Taniguchi, K., Desselberger, U., Van Ranst, M., 2008b. Recommendations for the classification of group A rotaviruses using all 11 genomic RNA segments. Arch. Virol. 153, 1621–1629.

Matthijnssens, J., Heylen, E., Zeller, M., Rahman, M., Lemey, P., Van Ranst, M., 2010a. Phylodynamic analyses of rotavirus genotypes G9 and G12 underscore their potential for swift global spread. Mol. Biol. Evol. 27, 2431–2436.

Matthijnssens, J., Otto, P.H., Ciarlet, M., Desselberger, U., Van Ranst, M., Johne, R., 2012. VP6-sequence-based cutoff values as a criterion for rotavirus species demarcation. Arch. Virol. 157, 1177–1182.

Matthijnssens, J., Rahman, M., Ciarlet, M., Zeller, M., Heylen, E., Nakagomi, T., Uchida, R., Hassan, Z., Azim, T., Nakagomi, O., Van Ranst, M., 2010b. Reassortment of human rotavirus gene segments into G11 rotavirus strains. Emerg. Infect. Dis. 16, 625–630.

Mossel, E.C., Ramig, R.F., 2003. A lymphatic mechanism of rotavirus extraintestinal spread in the neonatal mouse. J. Virol. 77, 12352–12356.

Pager, C., Steele, D., Gwamanda, P., Driessen, M., 2000. A neonatal death associated with rotavirus infection-detection of rotavirus dsRNA in the cerebrospinal fluid. S. Afr. Med. J. 90, 364–365.

Park, S.J., Kim, G.Y., Choy, H.E., Hong, Y.J., Saif, L.J., Jeong, J.H., Park, S.I., Kim, H.H., Kim, S.K., Shin, S.S., Kang, M.I., Cho, K.O., 2007. Dual enteric and respiratory tropisms of winter dysentery bovine coronavirus in calves. Arch. Virol. 152, 1885–1900.

Petersen, C., Kuske, M., Bruns, E., Biermanns, D., Wussow, P.V., Mildenberger, H., 1998. Progress in developing animal models for biliary atresia. Eur. J. Pediatr. Surg. 8, 137–141.

Phan, T.G., Okitsu, S., Maneekarn, N., Ushijima, H., 2007. Genetic heterogeneity, evolution and recombination in emerging G9 rotaviruses. Infect. Genet. Evol. 7, 656–663.

Ramig, R.F., 2004. Pathogenesis of intestinal and systemic rotavirus infection. J. Virol. 78, 10213–10220.

Riepenhoff-Talty, M., Gouvea, V., Evans, M.J., Svensson, L., Hoffenberg, E., Sokol, R.J., Uhnoo, I., Greenberg, S.J., Schäkel, K., Zhaori, G., Fitzgerald, J., Chong, S., el-Yousef, M., Nemeth, A., Brown, M., Piccoli, D., Hyams, J., Ruffin, D., Rossi, T., 1996. Detection of group C rotavirus in infants with extrahepatic biliary atresia. J. Infect. Dis. 174, 8–15.

Santos, N., Hoshino, Y., 2005. Global distribution of rotavirus serotypes/genotypes and its implication for the development and implementation of an effective rotavirus vaccine. Rev. Med. Virol. 15, 29–56.

Shepherd, R.W., Butler, D.G., Cutz, E., Gall, D.G., Hamilton, J.R., 1979. The mucosal lesion in viral enteritis. Extent and dynamics of the epithelial response to virus invasion in transmissible gastroenteritis of piglets. Gastroenterology 76, 770–777.

Snodgrass, D.R., Ferguson, A., Allan, F., Angus, K.W., Mitchell, B., 1979. Small intestinal morphology and epithelial cell kinetics in lamb rotavirus infections. Gastroenterology 76, 477–481.

Tate, J.E., Burton, A.H., Boschi-Pinto, C., Steele, A.D., Duque, J., Parashar, U.D., WHO-coordinated Global Rotavirus Surveillance Network, 2012. 2008 estimate of worldwide rotavirus-associated mortality in children younger than 5 years before the introduction of universal rotavirus vaccination programmes: a systematic review and meta-analysis. Lancet Infect. Dis. 12, 136–141.

Timenetsky, M.D.C., Santos, N., Gouvea, V., 1994. Survey of rotavirus G and P types associated with human gastroenteritis in Sao Paulo, Brazil, from 1986 to 1992. J. Clin. Microbiol. 32, 2622–2624.

Unicomb, L.E., Podder, G., Gentsch, J.R., Woods, P.A., Hasan, K.Z., Faruque, A.S., Albert, M.J., Glass, R.I., 1999. Evidence of high-frequency genomic reassortment of group A rotavirus strains in Bangladesh: emergence of type G9 in 1995. J. Clin. Microbiol. 37, 1885–1891.

Varghese, V., Das, S., Singh, N.B., Kojima, K., Bhattacharya, S.K., Krishnan, T., Kobayashi, N., Naik, T.N., 2004. Molecular characterization of a human rotavirus reveals porcine characteristics in most of the genes including VP6 and NSP4. Arch. Virol. 149, 155–172.

Zeller, M., Heylen, E., De Coster, S., Van Ranst, M., Matthijnssens, J., 2012. Full genome characterization of a porcine-like human G9P[6] rotavirus strain isolated in Belgium. Infect. Genet. Evol. 12, 1492–1500.

Zheng, B.J., Chang, R.X., Ma, G.Z., Xie, J.M., Liu, Q., Liang, X.R., Ng, M.H., 1991. Rotavirus infection of the oropharynx and respiratory tract in young children. J. Med. Virol. 34, 29–37.

Zhao, W., Xia, M., Bridges-Malveo, T., Cantú, M., McNeal, M.M., Choi, A.H., Ward, R.L., Sestak, K., 2005. Evaluation of rotavirus dsRNA load in specimens and body fluids from experimentally infected juvenile macaques by real-time PCR. Virology 341, 248–256.